ISSN: 0067-2904

Calculating Parameters for Se and Tin Plasmas Produced by Pulsed Nd: YAG Laser

Zahraa A. Saeed, Kadhim A. Aadim*
Department of Physics, College of Science, University of Baghdad, Baghdad, Iraq

Received: 8/2/2022 Accepted: 8/8/2022 Published: 30/3/2023

Abstract

In this study, the plasma formed by the preparation of Se and Tin (Sn) using a Nd: YAG laser with a wavelength of 1064 nm in air, which was then studied using the technique of optical emission spectrum, was presented (OES).The laser-induced plasma parameters such an electron temperature (Te) were identified using two-ratio methods, using Stark broadening methods to determine the density of electrons (n_e). According to the findings, there is a correlation between the amount of laser energy that is applied and the increase in the emission intensity of the spectral lines. In the case of Se plasma, an increase in laser energy causes a rise in the temperature of the electrons. While increasing the temperature of the electrons by increasing the amount of laser energy, the temperature of the Sn plasma gradually lowers. By increasing the laser energy, the electron density of both selenium (Se) and tin (Sn) can be increased. In addition, the parameters of the plasma were discovered. Such parameters as the Debye length (λ_D), plasma frequency (F_p), and Debye Number (N_D).

Keywords: Selenium (Se), Tin (Sn), Optical Emission Spectroscopy (OES), Nd: YAG laser, Laser-Induced Breakdown Spectroscopy (LIBS).

حساب معلمات البلازما للعناصر Se و Tin (Sn) المنتجة بواسطة الليزر النبضي Nd: YAG

زهراء عبدالكريم سعيد ، كاظم عبدالواحد عادم*
قسم الفيزياء, كلية العلوم, جامعة بغداد, بغداد, العراق

الخلاصة:

في هذه الدراسة ، تم تقديم البلازما المتكونة من تحضير Se و Tin (Sn) بأستخدام ليزر Nd: YAG بطول موجة λ 1064 = نانومتر والتي تمت دراستها بعد ذلك بأستخدام تقنية طيف الانبعاث الضوئي (OES). تم تحديد معلمات البلازما المستحثة بالليزر مثل درجة حرارة الإلكترون (T_e) باستخدام طريقة النسبة الثنائية ، وكثافة الإلكترون (n_e) بواسطة طرق توسيع ستارك .وفقا النتائج ,هناك علاقة بين كمية طاقة الليزر المطبقة و زيادة شدة انبعاث الخطوط الطيفية في حالة Seبلازما, تؤدي الزيادة في طاقة الليزر الى ارتفاع درجات حرارة الالكترونات. اثناء زيادة درجة حرارة الالكترونات عن طريق زيادة كمية طاقة الليزر , تنخفض درجة حرارة البلازما Tin(Sn) تدريجيا .عن طريق زيادة طاقة الليزر ,يمكن زيادة كثافة الالكترون لكل من Se و Tin (Sn).بالاضافة الى ذلك, تم اكتشاف معاملات البلازما الاخرى , ، مثل طول ديباي (λ_D) ، عدد ديباي (N_D) وتردد البلازما (F_P). تظهر جميع معلمات البلازما تتأثر بطاقة الليزر.

*Email: kadhim_adem@scbaghdad.edu.iq

1. Introduction

Optical emission spectroscopy (OES) is the simplest hardware technology, and it is one of the plasma diagnostics tools that have been used for industrial applications, and this technology is used to find the spectrum produced by the plasma produced by Nd:YAG laser in air, with $\lambda = 1064$ nm [1].

Laser induced breakdown spectroscopy (LIBS) is a technique that uses high-energy laser pulses of atomic emission spectroscopy to excite optical samples. Generating of plasma by high energy laser pulse's reaction with a metal surface to analyze [2].
Analytical plasma is stimulated when vaporized and excited by laser pulses during bombardment of the target element [3].

When the laser is applied on the sample, it evaporates and ionizes in small quantities. In addition, this technique is an important method for quickly determining or detecting the composition of the sample and it also used to analyze any type of material, whether in the solid, liquid, or gaseous state[4].

The primary studies on the principles and emission of the LIBS technique involve two parts. The first part includes studies plasma parameters and laser-material interaction studies plasma parameters, such as sample material physical parameters and laser properties. The second part studies mechanisms for plasma. Development that depend on space and time [5].
Selenium (Se) is present in a small amount in rock-forming minerals and it is considered one of the main pollutants of the environment, as the biochemical cycle of selenium has not yet been identified but is dominant by microorganisms which play a crucial role in methylation, volatilization, and reduction-oxidation.Se oxyanions (selenate and selenite) dominate in aqueous systems can be reduced by microbes (enzymatically, or indirectly) to comparatively insoluble, immobile, and non-toxic forms (e.g. Se°) [6].

Tin (Sn) is found in igneous rocks in the earth's crust and is similar to technically useful elements such as copper, cobalt, lead, nickel, and cerium and is essentially equal to the abundance of nitrogen [7].

In antiquity, the origin of tin (Sn) was lost. When pure tin was not yet isolated and used for specific purposes, people turned to bronze, which is Tin (Sn) alloy mixed with copper that may be found in a wide variety of products today, including food cans and bearings. Organ Tin (Sn) compounds, such as Vulgaris, which is used in fungicides and biocides that are hazardous to humans, are deemed non-toxic. Tin (Sn) on the other hand, is regarded toxic [8].

2. Materials and Methods

This study formed the plasma using a pulsed laser on the solid elements (Se and Sn).The experimental arrangement of the LIBS technique from shown in (Figure.1). The pulse laser (Nd: YAG) with a wavelength of 1064 nm and a frequency of 6Hz with the laser pulse energy varied from 400 to 700mJ was used to generate the plasma. The target material laser beam was concentrated on the target, making a (45°) angle with it In order to obtain the largest surface area of the element on which the laser focuses. Optical emission spectroscopy (OES) was used to determine the electron's temperature, plasma frequency, and densities. When the findings were compared to those in the NIST database, it was found that there was no significant difference between the two sets of data [9].

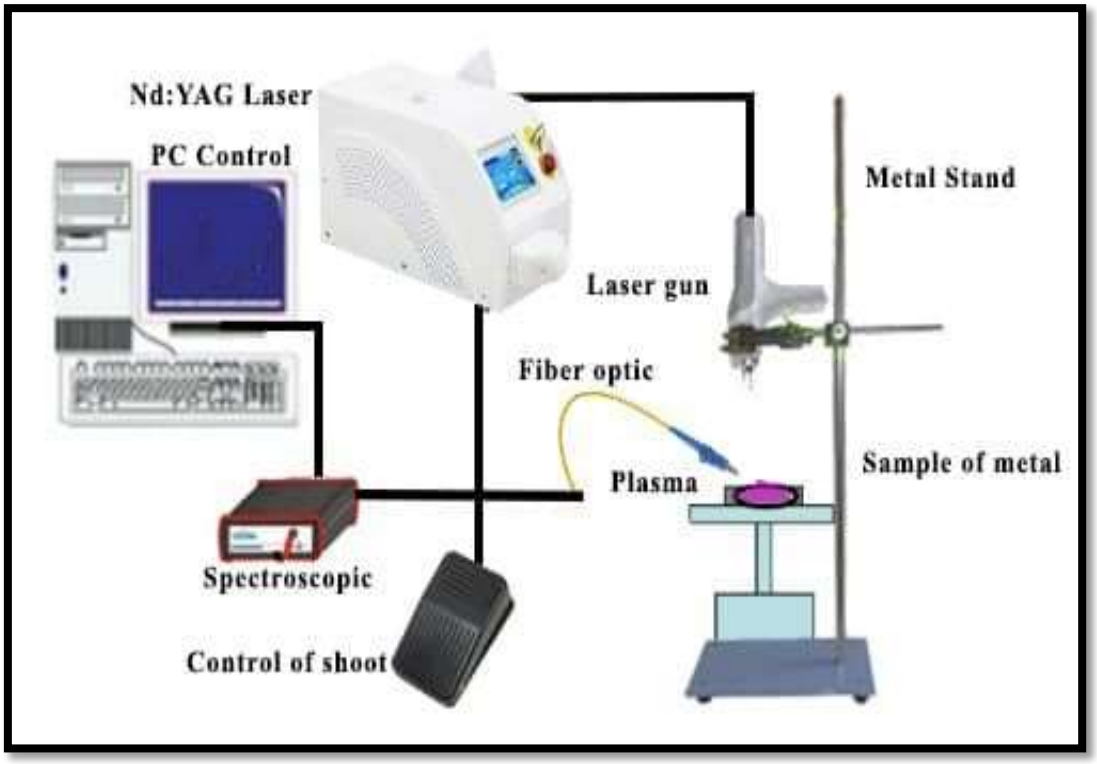

Figure 1: Laser-Induced Breakdown Spectroscopy (LIBS) System Configuration

3. Covering equations

The electron temperature (Te) can be determined from the following expression[10].

$$\frac{I_1}{I_2} = \frac{g_1 A_1 \lambda 2}{g_2 A_2 \lambda 1} \; exp \left[- \frac{E1 - E2}{K T_e} \right] \qquad \text{..... (1)}$$

Where: I is the intensity, λ is the wavelength, g is the statistical weight, A is the transition probability, E is the energy of the excited level of these spectral lines, T_e is the electron temperature, and K is the Boltzmann constant.

The electron density can be estimated depending on the spectral line widths through the following relation [11].

$$n_e = \left(\frac{\lambda_{FWHM}}{2_w}\right) \times 10^{16} \qquad \text{..... (2)}$$

Where n_e is the electron density [cm^{-3}] ,λ_{FWHM} refers to the Stark full-width at half-maximum, and w is the electron impact parameter.

Evaluate plasma frequency (F_p) by the equation [12].

$$f_p = \frac{w_p}{2\pi} \quad \text{and} \quad w_p = \left(\frac{n_e \, e^2}{\varepsilon_\circ m_e}\right)^{1/2} \qquad \text{..... (3)}$$

Where m_e is the electron rest mass .

The Debye length (λ_D) in cm from the following equation [12].

$$\lambda_D = \left(\frac{\varepsilon_\circ k_B T_e}{n_e \; e^2}\right)^{1/2} = 743 \sqrt{\frac{T_e}{n_e}} \qquad \text{..... (4)}$$

Where $\varepsilon_\circ$ is the vacuum permittivity, k_B is Boltzmann constant, and e is the electron charge.

The Debye number (N_D) can also be calculated from the following equation [12].

$$N_D = \frac{4\pi n_e}{3} (\lambda_D)^3 \quad \text{..... (5)}$$

4. RESULT AND DISCUSSIONS

4.1. Description of the Emission Spectra

In this study, the plasma emission generated by the fundamental wavelength (1064nm) of the Q-switched Nd: YAG laser was studied. The set of experiments with the 1064 nm laser focused on the selenium and Tin (Sn) surfaces and the emission spectra of the respective plasma were recorded. The target material was evaporated and ionized by a laser beam, forming a plasma plume on the target surface. The emission spectra of the laser-generated selenium and Tin (Sn) plasma are produced depicted in Figures 2 and 3 respectively, space the spectral area from 200–700 nm. These spectra may be found in the spectral region from 200–700 nm. The most notable Se spectral lines are shown in (Figure 2) as Se I (at 475.5276 nm), Se I (at 587.2707 nm), Se II (at 407.545 nm), and Se II (at597.893 nm).

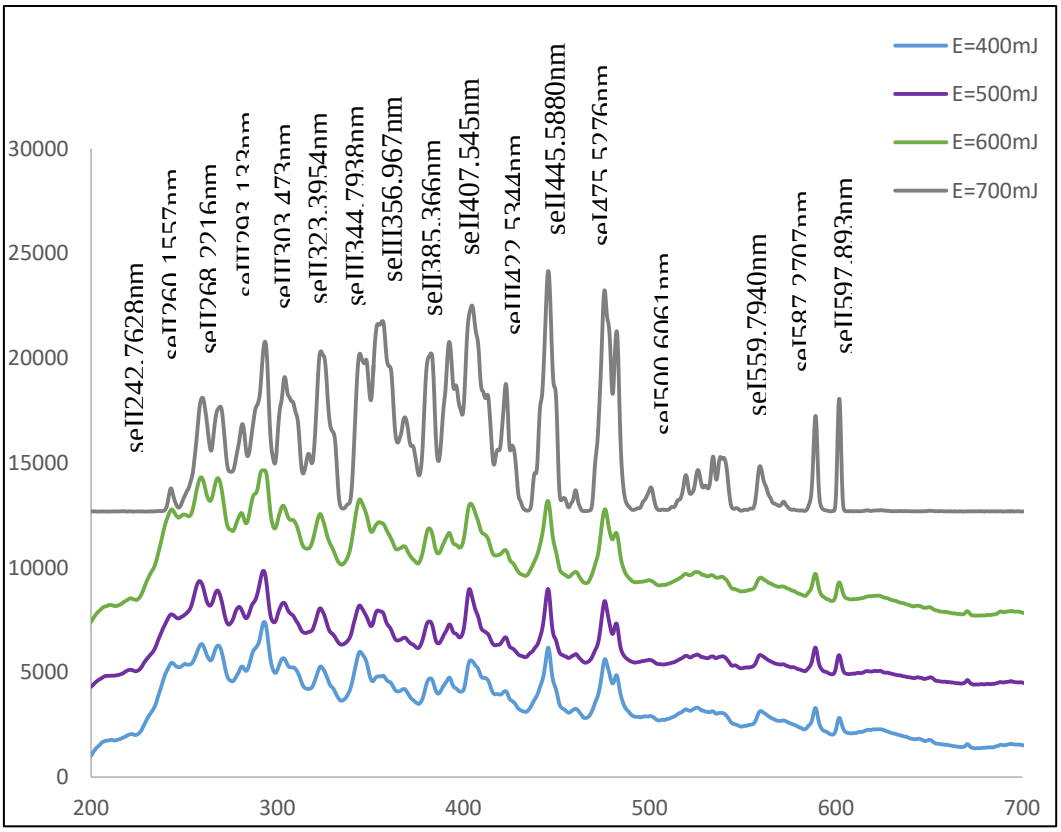

Figure 2: The plasma emission spectra of Se target as a function of energy.

(Figures 3) show the prominent Sn spectral lines are Sn I (at 283.99765 nm), Sn I (at 452.47344 nm), Sn II (at 479.20732 nm), and Sn II (at 656.97 nm). These transitions of two elements are identified by using the spectral database of the National Institute of Standards and Technology (NIST) [9]

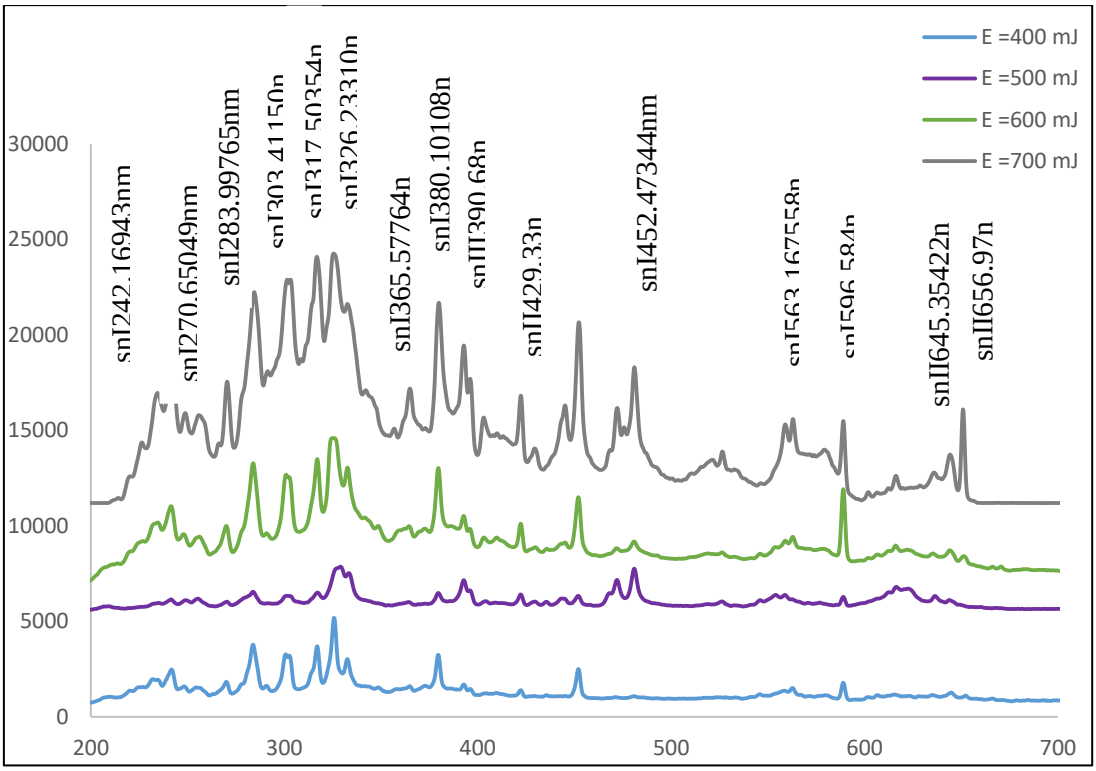

Figure 3: The plasma emission spectra of Tin (Sn) target as a function of energy.

In this work, the intensities of Se II lines at 268.2216 nm and 597.893 nm are measured at different laser energy. Figure 3 shows the effect of laser energy on emission lines intensities. When the laser energies increase, we observed an increase in the spectral emission lines of the element due to the increase in the extraction of electrons and the occurrence of the ionization process, and an increase in the plasma absorption of laser photon .

4.2. Electron temperature measure.

Electron temperature (Te) was determined by Equation (1); its changes with laser energy for selenium and tin targets are shown in Figure 4 and Figure 5, respectively. As the plasma approaches maximum expansion velocities, the thermal energy is rapidly converted to kinetic energy, causing an increase in the plasma temperature. This result agrees with Mohammed et al. [13]and Qindeel et al. [14]. But in (550 nm) to (600 nm), the decreasing in temperature is due to the rapid transformation of thermal energy into kinetic energy when the plasma expands [15][16]. While Figure 5 shows the temperature of tin (Sn) is seen to increase in the spectral range of (350 nm-550nm) while a slow variation of electron temperature was seen for the spectral range(600 nm-750 nm) [14].

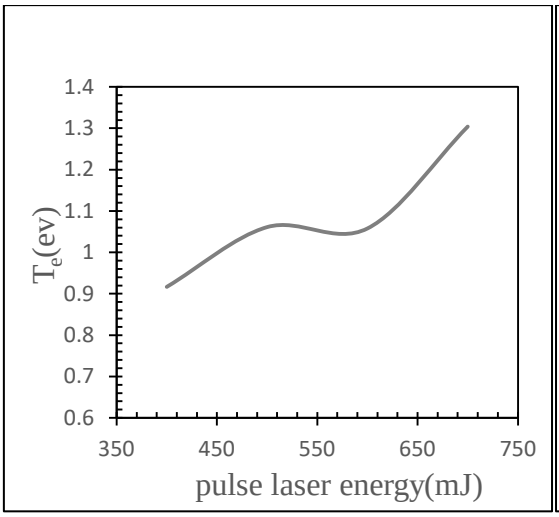

Figure 4: Electron Temperature of Se.

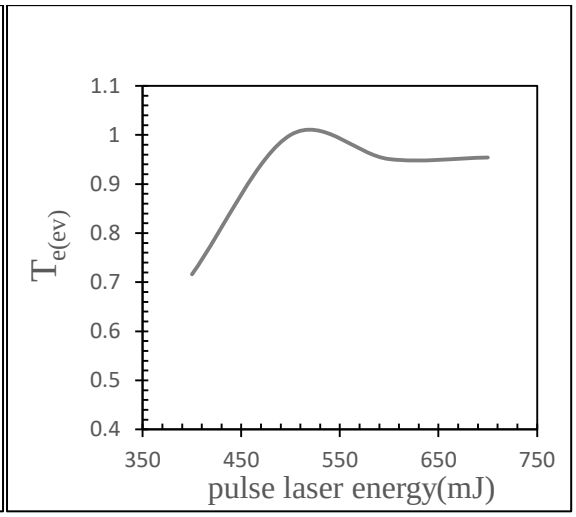

Figure 5: Electron Temperature of Tin (Sn).

4.3. Electron density measure.

The electron density was estimated depending on the spectral line widths through Equation (2). Figures 6 and 7 show the changes of the electron density for the selenium (Se) element and the tin (Sn) element, respectively as a function of laser power. It is noted that the electron density for both elements increases as the laser power increases. This led the temperature to rise.

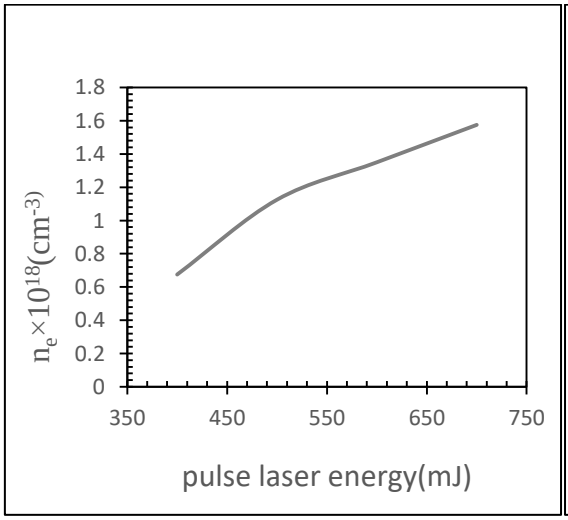

Figure 6: Electron Density of Se.

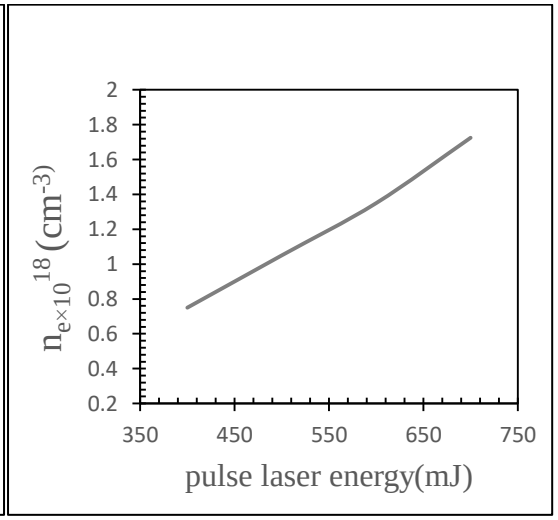

Figure 7: Electron Density of Tin (Sn)

4.4. Other plasma parameters (plasma frequency, Debye length and, Debye number).

Plasma frequency(F_p) was evaluated using Equation (3), and it was plotted as a function of laser power (Figures 8 and 9. It was observed that the plasma frequency rises for both the selenium (Se) element and the Tin (Sn) element when there is an increase in the laser power.

The Debye length (λ_D) is measured in centimeters from the following equation (4). Figures 10 and 11 represent the Debye length for both selenium and tin with increasing energy.

The Debye number (N_D) can also be calculated from the following equation (5). Figures 12 and 13 represent the Debye number for both selenium and tin with increasing laser power.

Table 1 represents the plasma parameters of Se with different laser power.
The second table represents the plasma parameters for tin with different laser power.

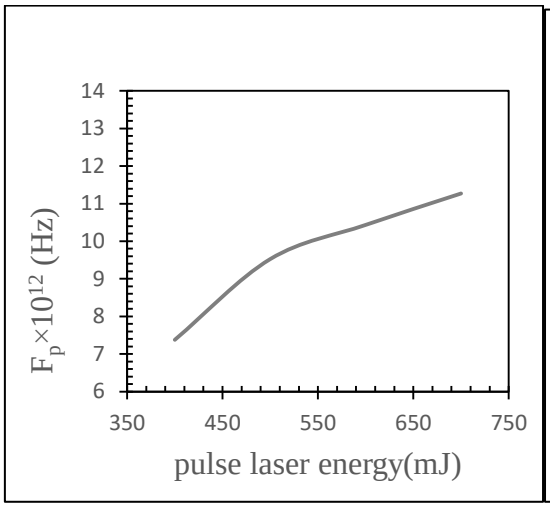

Figure 8: plasma frequency of Se.

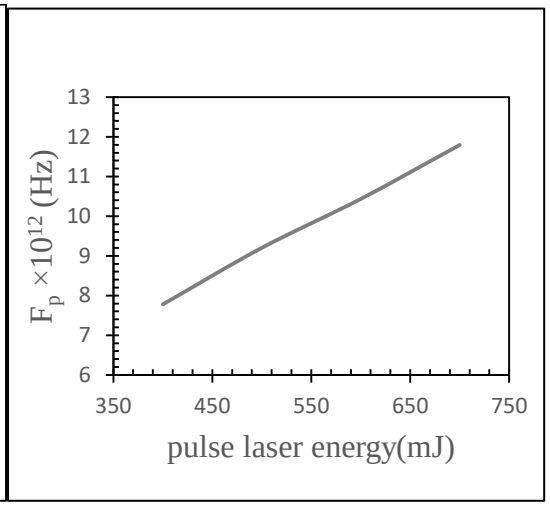

Figure 9: plasma frequency of Tin (Sn).

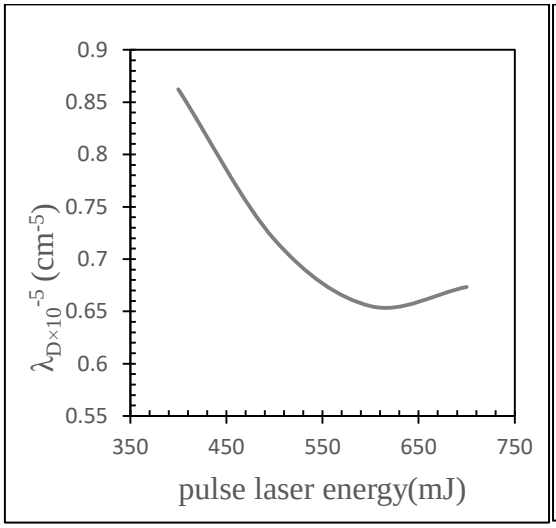

Figure 10: Debye length of Se.

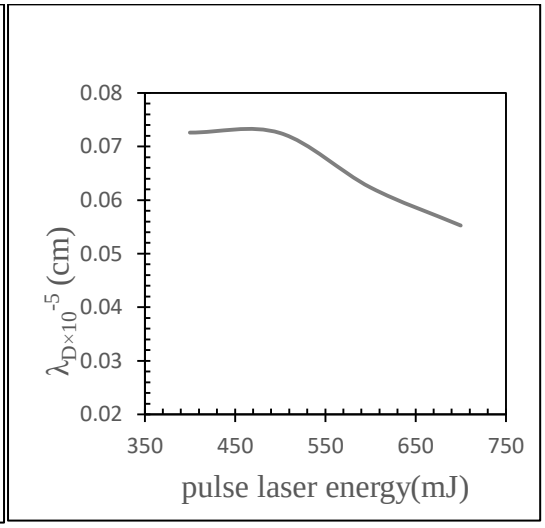

Figure 11: Debye length of Tin (Sn).

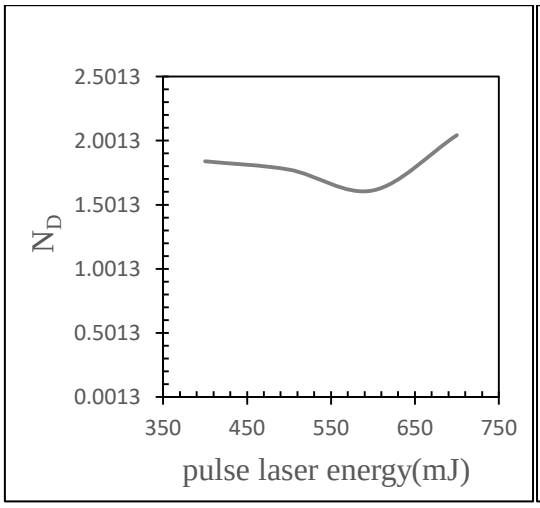

Figure 12: Debye number of Se.

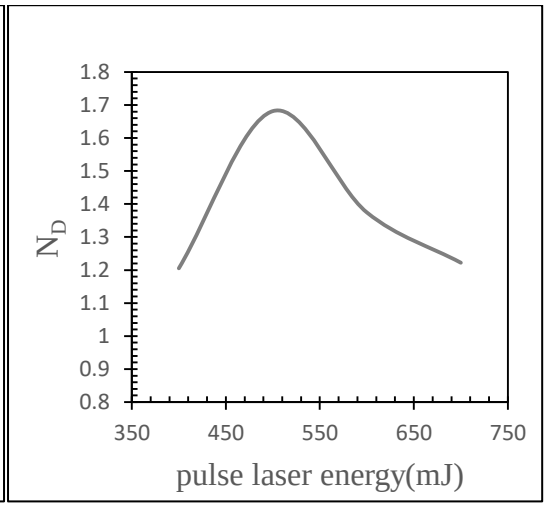

Figure 13: Debye number of Tin (Sn).

Table 1: plasma parameters for Se with laser different energy

E (mJ)	T_e (eV)	$n_e \times 10^{18}$ (cm^{-3})	$f_p \times 10^{12}$ (Hz)	$\lambda_D \times 10^{-5}$(cm)	N_d (cm^{-3})
400	0.917	0.68	7.378	0.087	1.840
500	1.061	1.13	9.525	0.072	1.775
600	1.058	1.35	10.434	0.066	1.613
700	1.304	1.58	11.270	0.068	2.044

Table 2: plasma parameters for Tin (Sn) with laser different energy.

E (mJ)	T_e (eV)	$n_e \times 10^{18}$ (cm^{-3})	$f_p \times 10^{12}$ (Hz)	$\lambda_D \times 10^{-5}$(cm)	N_d (cm^{-3})
400	0.716	0.75	7.777	0.073	1.205
500	1.000	1.05	9.202	0.073	1.681
600	0.951	1.35	10.434	0.062	1.375
700	0.954	1.73	11.794	0.055	1.222

5. Conclusion:

Finding the plasma emission produced by the Q-switched Nd: YAG pulsed laser on Tin (Sn) and Se elements by basic wavelength 1064 nm in the air at atmospheric pressure has been accomplished by the use of the optical emission spectrum (OES) method. In this study, the properties of the plasma as well as the effect of the laser energy on it were explored at various laser energies ranging from 400 to 700 mJ. The two wavelengths in ratio approach was utilized in the determination of the electron temperature, and the Stark broadening methods for spectral lines were utilized for the computation of the electron density. The energy of the laser causes a rise in the intensity of the emission spectrum. In selenium (Se) plasma, the temperature of the electrons rises as the laser energy increases, whereas in tin (Sn) plasma, the temperature first rises and then falls. When the laser intensity is raised, there is a corresponding increase in the electron density for both Se and Tin (Sn). On the other hand, laser energy has an effect on all of the plasma parameters, including the Debye length (D) and the plasma frequency (Fp), as can be seen in Figures 8 and 9.

6. ACKNOWLEDGMENTS

We thank Plasma Physics Lab., Physics Department, College of Science, University of Baghdad, for supporting this work.

7. REFERENCES

[1] M. M. Shehab and K. A. Aadim, "Spectroscopic Diagnosis of the CdO: CoO Plasma Produced by Nd: YAG Laser," *Iraqi J. Sci.*, pp. 2948–2955, 2021.

[2] A. Hayat *et al.*, "The role of spatial confinement for improvement of laser-induced Mg plasma parameters and growth of surface features," *Appl. Phys. A*, vol. 123, no. 8, pp. 1–17, 2017.

[3] K. A. Aadim, "Detection of laser-produced tin plasma emission lines in atmospheric environment by optical emission spectroscopy technique," *Photonic Sensors*, vol. 7, no. 4, pp. 289–293, 2017.

[4] G. Galbács, V. Budavári, and Z. Geretovszky, "Multi-pulse laser-induced plasma spectroscopy using a single laser source and a compact spectrometer," *J. Anal. At. Spectrom.*, vol. 20, no. 9, pp. 974–980, 2005.

[5] J. R. Freeman, S. S. Harilal, P. K. Diwakar, B. Verhoff, and A. Hassanein, "Comparison of optical emission from nanosecond and femtosecond laser produced plasma in atmosphere and vacuum conditions," *Spectrochim. Acta Part B At. Spectrosc.*, vol. 87, pp. 43–50, 2013.

[6] S. C. Fakra, *Spectro-microscopic studies of microbial selenium and iron reduction in a metal contaminated aquifer*. University of California, Berkeley, 2015.
[7] H. G. Dill, R. Botz, Z. Berner, M. B. Abdullah, and A. Hamad, "The origin of pre-and synrift, hypogene Fe-P mineralization during the Cenozoic along the Dead Sea Transform Fault, Northwest Jordan," *Econ. Geol.*, vol. 105, no. 7, pp. 1301–1319, 2010.
[8] A. Moura and J. L. Velho, *Recursos geológicos de Portugal*. 2012.
[9] Y. Ralchenko, "NIST atomic spectra database.," *Mem. della Soc. Astron. Ital. Suppl.*, vol. 8, p. 96, 2005.
[10] E. R. Wainwright, S. W. Dean, F. C. De Lucia, T. P. Weihs, and J. L. Gottfried, "Effect of sample morphology on the spectral and spatiotemporal characteristics of laser-induced plasmas from aluminum," *Appl. Phys. A*, vol. 126, no. 2, pp. 1–18, 2020.
[11] M. Fikry, W. Tawfik, and M. M. Omar, "Investigation on the effects of laser parameters on the plasma profile of copper using picosecond laser induced plasma spectroscopy," *Opt. Quantum Electron.*, vol. 52, no. 5, pp. 1–16, 2020.
[12] A. Piel, *Plasma physics: an introduction to laboratory, space, and fusion plasmas*. Springer, 2017.
[13] R. Qindeel, M. S. Dimitrijević, N. M. Shaikh, N. Bidin, and Y. M. Daud, "Spectroscopic estimation of electron temperature and density of zinc plasma open air induced by Nd: YAG laser," *Eur. Phys. Journal-Applied Phys.*, vol. 50, no. 3, 2010.
[14] R. S. Mohammed, K. A. Aadim, and K. A. Ahmed, "Laser Intensity and Matrix Effect on Plasma Parameters for CuZn, Cu, and Zn Produced by Nd: YAG Laser," *Acta Phys. Pol. A.*, vol. 140, no. 4, 2021.
[15] K. A. Ahmed, K. A. Aadim, and R. S. Mohammed, "Investigation the energy influence and excitation wavelength on spectral characteristics of laser induced MgZn plasma," in *AIP Conference Proceedings*, 2021, vol. 2372, no. 1, p. 80004.
[16] Q. A. Abbas, "Effect of Target properties on the Plasma Characteristics that produced by Laser at Atmospheric Pressure," *Iraqi J. Sci.*, pp. 1251–1258, 2019.